Analysis of an Electric Vehicle with a BLDC PM Motor in the Wheel Body

K. Buhr * & P. Voženílek
Czech Technical University in Prague, Faculty of Electrical Engineering, Czech Republic
** Corresponding author: buhr@fel.cvut.cz*

DOI: 10.2478/v10158-012-001-8

ABSTRACT: The paper deals with the conception of the test bed for the permanent magnet brushless DC motor (PM BLDC) with parameter verification. The tested motor is destined for installation in the wheel body. The test bed HW and SW equipment is described in the paper. This equipment enables the automated measuring of load-rise, temperature-rise, and retardation tests. The test's aim is to obtain attested specifications for a vehicle dimensioning methodology design based on the knowledge of its dynamic behaviour and the track grading, and eventually of its energy consumption, action radius, etc.

KEYWORDS: electromobility, BLDC (brushless direct current), NdFeB, PM (permanent magnet), PWM (pulse width modulation) converter.

1 INTRODUCTION

The current basic candidates for an electrical vehicle's propulsion system are induction motors (IM), switched reluctance motors (SRM) and PM brushless motors (BLDC). The above-mentioned motors' active parts disposition is shown in mutual comparison in Fig. 1. Table 1 thereafter presents their quantitative confrontation (Gieras & Wing, 2002).

Table 1: Comparison of electric vehicle propulsion systems.

		IM	SRM	PM BLDC
specific output power	kW / kg	0.7	1.7	1.2
specific volume	10^4 x m^3 / kW	1.8	2.6	2.3
Efficiency	%	93.5	93	95.2
Overload capacity	-	2.4	1.9	2.2
torque ripple	%	7.3	24	10
maximum speed	rpm	12500	12500	9500

The main advantages of cage induction motors in Fig.1a are:

- simple construction
- simple maintenance (a standard maintenance routine concerns the sliding contacts in 90 % of cases)
- no commutator or slip rings
- low price and moderate reliability

The disadvantages of cage induction motors are:

- small air gap
- possibility of cracking the rotor bars due to hot spot at plugging and reversal
- lower efficiency

On the other hand the use of PM brushless motors (BLDC) has become a more attractive option compared to induction motors thanks to the following mains benefits:

- increase in the efficiency caused by non existing field excitation losses
- higher torque and output power per volume
- better dynamic behaviour
- simplification of construction and maintenance
- reduction of price for some types of machines

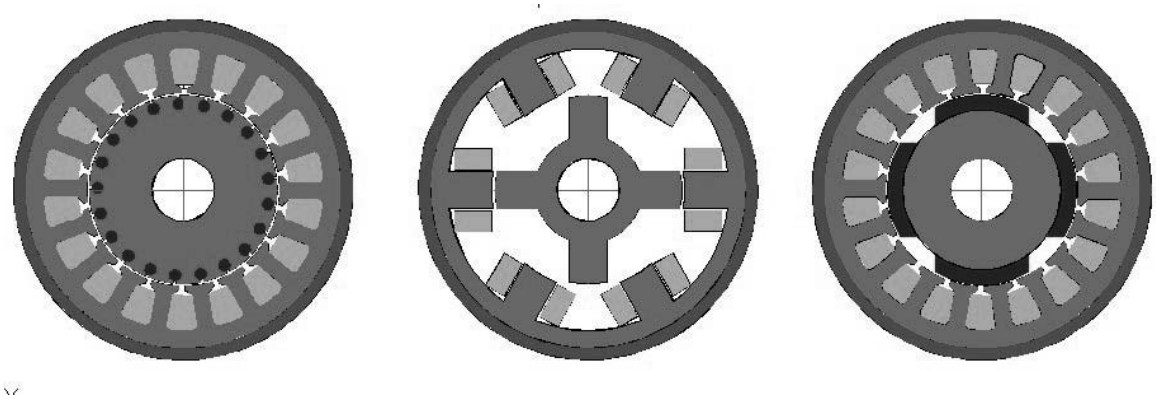

a) **b)** **c)**

Figure 1: Active parts a) induction motor, b) switched reluctance motor, c) PM brushless motor.

The power losses in PM brushless motors (Fig. 1.c) occur mainly in the stator where heat can be easily transferred through the ribbed frame, or in larger machines, a water cooling system can be used. PM brushless motor drives show the best output power to mass factor, efficiency, and compactness. PM d-c brushless and a-c synchronous motors are practically the same, with polyphase stator windings and PMs located on the rotor. The only difference is in the control and shape of the excitation voltage. A synchronous motor is fed with a more or less sinusoidal voltage which produces a rotating magnetic field. The armature current in BLDC motor has the shape of a square or trapezoidal waveform. Only two phase winding conduct the current at the same time. The switching pattern is synchronized with the rotor angular position (electronic commutation). In both types, the synchronous and brushless

motors' transmission of armature current is not transmitted by sliding contacts. An important advantage is also the fact that power losses occur only in the stator, where heat transfer conditions are good. Consequently, the current density can be increased, in comparison to a classical commutator d-c motor and, in addition, considerable improvements in dynamics can be achieved due to the air gap magnetic flux density being high and the rotor having a lower inertia; there are also no speed-dependent current limitations. The volume reduction of the BLDC motor in comparison with a classical commutator motor with PM can be as much as 40 %.

2 TYPICAL REALIZATION OF THE wheel body BLDC MOTOR

Modern drive units of road vehicles are mostly engineered with a magnetic circuit excited by permanent magnets in an axial or radial arrangement. The rotor is formed by the outer frame with the PM, the stator armature winding is built by the laminated magnetic core with the three-phase winding in slots. The winding is in a star or delta connection with terminals which are led out through a hollow shaft, see Fig.2. The number of slots per pole and phase is usually $q = 1$.

Control is realized by the three-phase PWM converter in a synchronous mode by Hall probes placed in the stator teeth. The general advantage of electrical vehicle drive, i.e., a multiple overload capacity in comparison with the combustion engine, is mentioned in the literature. However, this statement is valid only up to a certain point. Current rotating machines are produced usually in the insulation class F and H, and so a steady-state temperature rise could theoretically reach up to 150° C in class F and even 180° C in class H. However, the deciding factor, from the point of view of the vehicle drive dimensioning, is the NdFeB permanent magnet's maximal working temperature usually being 80 – 140° C. The permanent magnet's maximal temperature exceed threats with the machine demagnetization and herewith its non-reversible defect.

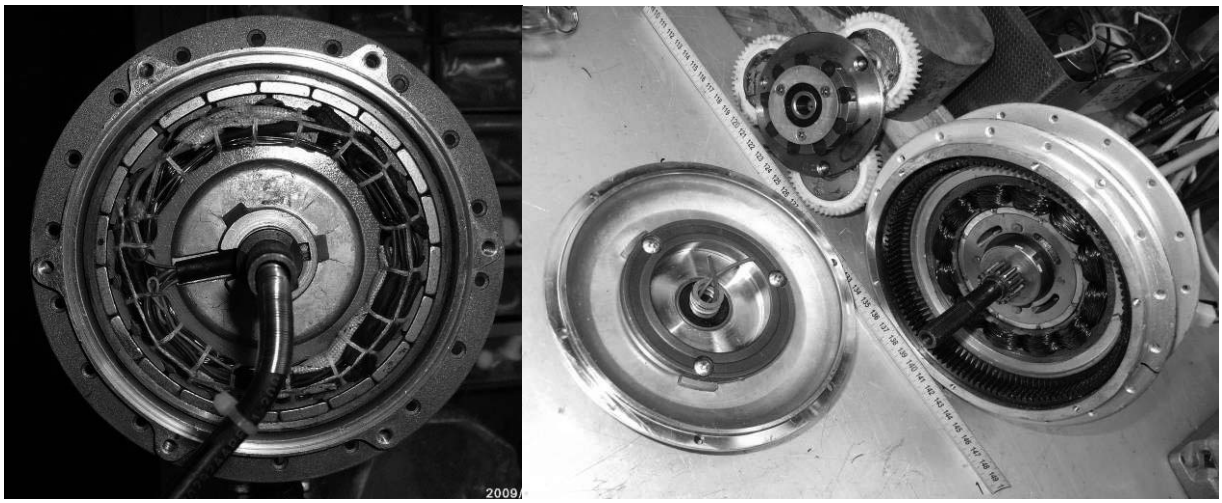

Figure 2:Comparison – construction of BLDC motors direct drive (left) and with planet gear (right).

Therefore, for the correct dimensioning of the vehicle drive it is essential to go out of the knowledge in thermal capacity of the actual BLDC motor and from the knowledge of vehicle working mode. In the case of the working mode, it is possible to go out from the passport of the European committee ENECE defining typical city traffic regime, see Fig. 3.

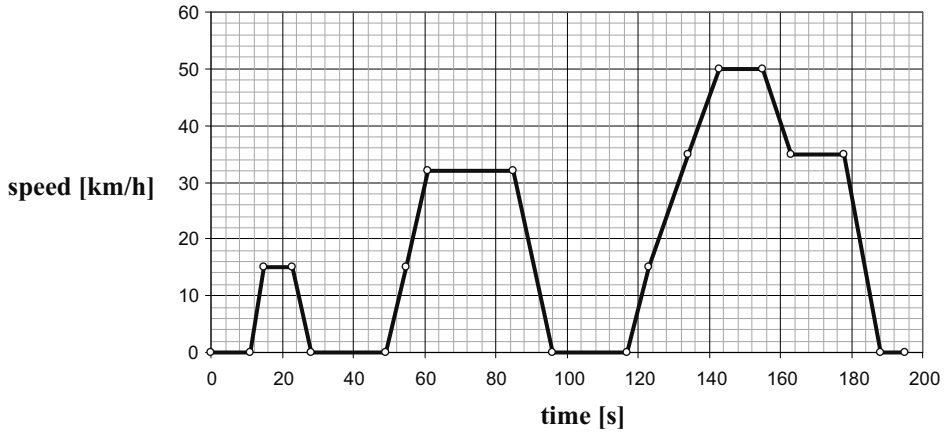

Figure 3: Typical city traffic regime by the ENECE 100.

It is obvious from the diagram that the mode of driving during acceleration and electro-dynamic braking has a major influence on the drive dimensioning. When it is not possible to take away the heat or arrange cooling in transient modes it is necessary to evaluate the drive dimensioning experimentally, for example on a vehicle model representing one axis or one wheel only.

3 DRIVE DIMENSIONING

Three fundamental types of road resistances have to be respected:

1. passive vehicle resistances
2. resistances for overcoming inertial forces of moving masses
3. resistances given by the profile of the track

Passive vehicle resistances have a main influence on running characteristics. They can be enumerated from:

a. Rolling resistances

$$F_{val} = o_{val} \cdot m_{voz} \cdot g \qquad [\mathrm{N}, \mathrm{N \cdot kN^{-1}}, \mathrm{t}, \mathrm{m \cdot s^{-2}}]$$

where o_{val} is given in Tab.1:

Table 2: Rolling resistances.

Wheel type	Traffic road type	Rolling-resistance force [N·kN^{-1}]
Passenger vehicle diagonal tyre radial tyre	Asphalt track	 15 ÷ 22 12 ÷ 18
Motor-truck diagonal tyre radial tyre	Asphalt track	 10 ÷ 15 8 ÷ 12
Motor-truck	Terrain	150 ÷ 200
Motor-truck / tractor	Plump terrain (plough)	250 ÷ 500
Rail vehicle	Rail	0,3 ÷ 1

b. Axle bearing friction

$$F_L = o_L \cdot m_{voz} \cdot g \qquad [\text{N, N/kN , t , m/s}^2\ ]$$

The value of the coefficient of bearing rolling friction o_L depends on the speed, temperature, and pasting quality. Its value is given in the production catalogue.

c. Aerodynamic resistance

$$F_A = c_x \cdot S_{čel} \cdot \frac{\rho}{2} \cdot \left(\frac{v_R}{3{,}6}\right)^2 \qquad [\text{N, - , m}^2\text{, kg·m}^{-2}\text{, km·h}^{-1}]$$

The vehicle's nose form factor c_x and its cross sectional area $S_{čel}$ have a decisive influence on the aerodynamic resistance. The relative vehicle speed v_R has a considerable influence as well. Additionally air density play a role. Air density depends on the temperature and on atmospheric pressure. In European conditions, where - 25° C ÷ + 40° C and 98.5 ÷ 103.5 kPa are assumed, air density ρ is 1.326 kg·m^{-2}. Form factor $\mathbf{c_x}$ is given in Tab. 2.

Table 3: Vehicle nose form factor.

Vehicle Type	Nose form factor
One-track (bicycle/motor-cycle)	0.6 ÷ 1.2
Passenger vehicle	0.25 ÷ 0.4
Open passenger vehicle	0.5 ÷ 0.65
Van	0.4 ÷ 0.5
Motor-truck	0.8 ÷ 1.0

A summary of vehicle resistance F_V for the resistance given by the profile of the track neglected is:

$$F_V = F_{val} + F_L + F_A = A + B \cdot v + C \cdot v^2$$

It is therefore evident that passive vehicle resistances have generally a parabolic form which is considerably influenced by its geometry, mass, and running speed.

Track profile, namely slope α, positively influences the rolling resistance magnitude by the normal component of the gravity force, i.e., the magnitude of the first term A:

$$F_{val} = F_{val\cdot} \cdot \cos\alpha$$

The gravity force component $F_{g,}$ given by the summary vehicle mass $m,$ has to be added to the passive vehicle resistances F_V which the driving unit must overcome for the track slope.

$$F_g = m \cdot g \cdot \sin\alpha$$

Running resistances from acceleration (i.e., dynamical resistances) are influenced by vehicle rotating masses and by resistances given by the masses of the translation motion. For the drive dimensioning, it is advantageous to reduce both the passive and dynamical resistances to the motor shaft. Therefore, inertia masses have to be related to the wheel circumference and expressed in a form of moment of inertia as:

$$J_{cel} = J_P + m \cdot \left(\frac{d_{kol}}{2}\right)^2 \cdot \frac{1}{i^2 \cdot \eta} \qquad [\text{kgm}^2, \text{kg, m}] ,$$

where i is a ratio and η is a summary of the efficiency of the power transmission on the axletree or on the wheel circumference.

The determination of drive moments of inertia J_p can produce some problems, as it usually is not included in the catalogue specified parameters. One possible method is an experimental moment of inertia evaluation using the method of the retardation test, where the machine is disconnected from the load and time dependence on the speed is measured, see Fig.7.

The balance between inertia mass torque and braking torque given by the machine's losses exists in any time point. A specific problem of PM motors is the fact that machine iron losses take part on the breaking torque and must be extracted from the inertia mass power:

$$\Delta P = J_p \cdot \omega \cdot \frac{d\omega}{dt}$$

4 EXPERIMENTAL PARAMETER SPECIFICATION METHODS

The type of the tested BLDC motor is introduced in Fig.4. It is a low speed motor without an inbuilt gear box assigned for the individual drive of the motor car wheel (direct drive). The motor was installed with four screw bolts for direct wheel mounting and also with a disc brake. The drive was made in China and it was delivered without any specification of a particular production type and without any sheet parameters. The type's output was estimated in the range of between 1500 - 3000 W, supply voltage 48 V, any other information about the drive components and specifically of its converter is not known. The machine's mass of 18 kg was found by weighing it.

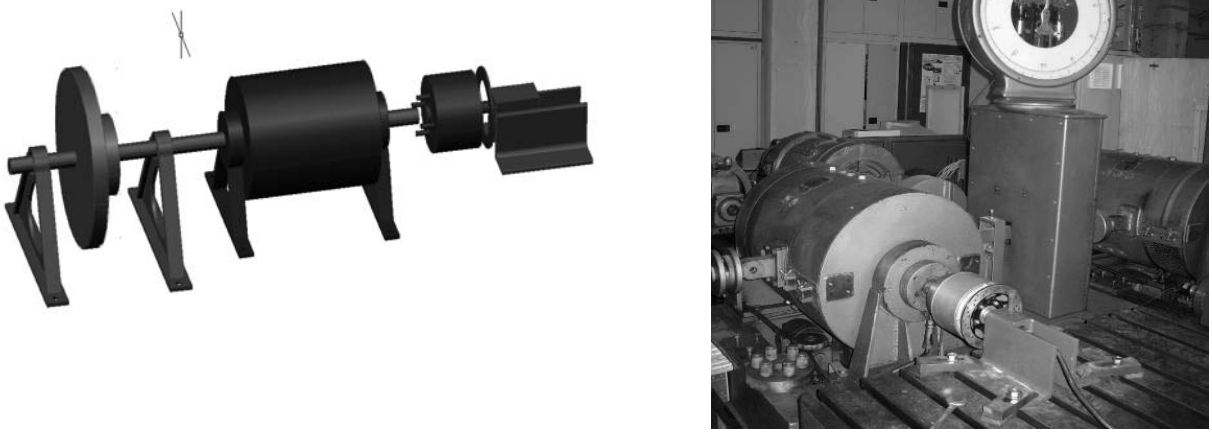

Figure 4: Front view of the workplace, mechanical coupling of motor – dynamometer.

Experiments were focused on parameter verification and on the drive dimensioning in terms of the ideas mentioned in the 2nd and 3rd chapter:

- method for the measurement verification of the drive's mechanical characteristics
- verification and realization of temperature-rise test for a steady state duty cycle
- verification of the methods for the moment of inertia measurement using the retardation test

The aim of the authors was to build an experimental workplace for experiments ona complete model of a vehicle's drive reduced to one wheel. The thinking is based on the fact that a vehicle's passive resistances can be replicated by the dynamometer load. The vehicle mass or its load can be replicated using a fly-wheel on the reverse side of the dynamometer, see Fig.4. Therefore load tests of any vehicle with a chosen driving cycle can be realized only on basis of the above-mentioned three tests.

5 DESCRIPTION OF THE WORKPLACE – TEST RESULTS

The base of the experimental workplace mechanical part includes:

- Dynamometer 50 kW, 200 Nm
- Ward-Leonard motor-generator set
- Set of fly-wheels

Unified instrumentation includes a power analyser NORMA 4000, equipped with ac/dc current LEM clip-on probes. The power analyser is connected by the series interface RS 232 to a PC installed with Norma X software for the transmission and storage of the measured data.

The motor's speed can be derived from the frequency of the armature induced voltage with regard to the control mode of the BLDC motor when the magnetic field rotates synchronously with the rotor. It is not necessary to install the speed indicator permanently.

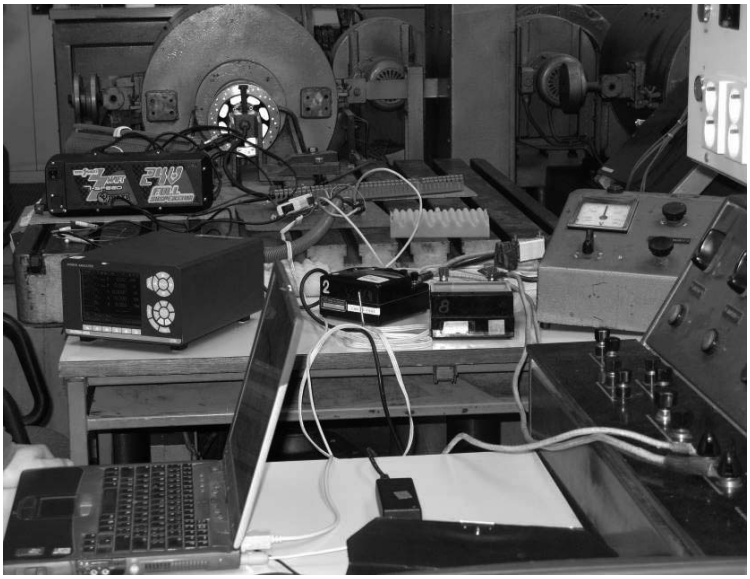

Figure 5: View of the improvised measuring workplace.

The measured torque-speed characteristic for the two different supply voltages, 55 V and 60 V d-c, is shown in Fig. 6. The values of the torque were so far read manually. Automated torque data collection will, in the future, be realised with a given rate, using the dynamometer armature current measurement. Regarding the suppressed speed-axis origin, see Fig. 6, it is possible to claim that motor is a sufficiently hard source of the mechanical power. The temperature-rise test was realized using the "Resistance Method" and is documented in the cooling curve shown in Fig.8. The machine was loaded with a constant load of 40 Nm at a speed of 665 min^{-1} until temperature stabilization, i.e., about 30 minutes. Then the converter was switched off and the winding of one phase was switched to the d-c source after about 4 minutes (accumulator 12 V).

The voltage and current were measured using a power analyser in about 6000 points and the resistance was calculated. The winding resistance was evaluated after the extrapolation of the cooling curve to the point of switch off time.

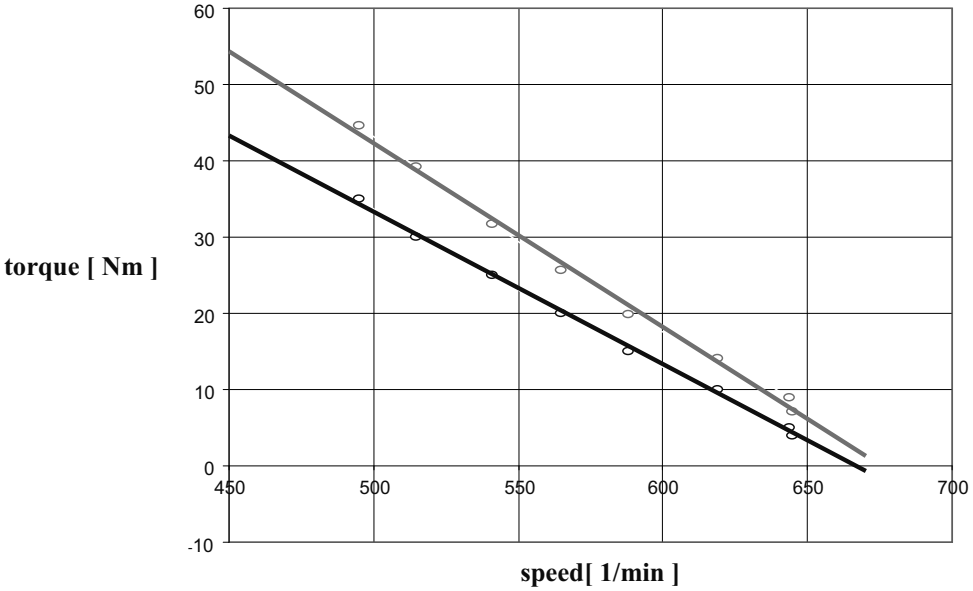

Figure 6: Torque-speed characteristic.

The winding temperature-rise was evaluated using the hot and cold resistance difference. The medium winding temperature-rise in this case was 51.6° C and the temperature was 71.1° C. That is tolerable from the point of view of the limit operation temperature of the permanent NdFeB magnets used. The machine's 30 minutes power was then determined as 2.8 kW.

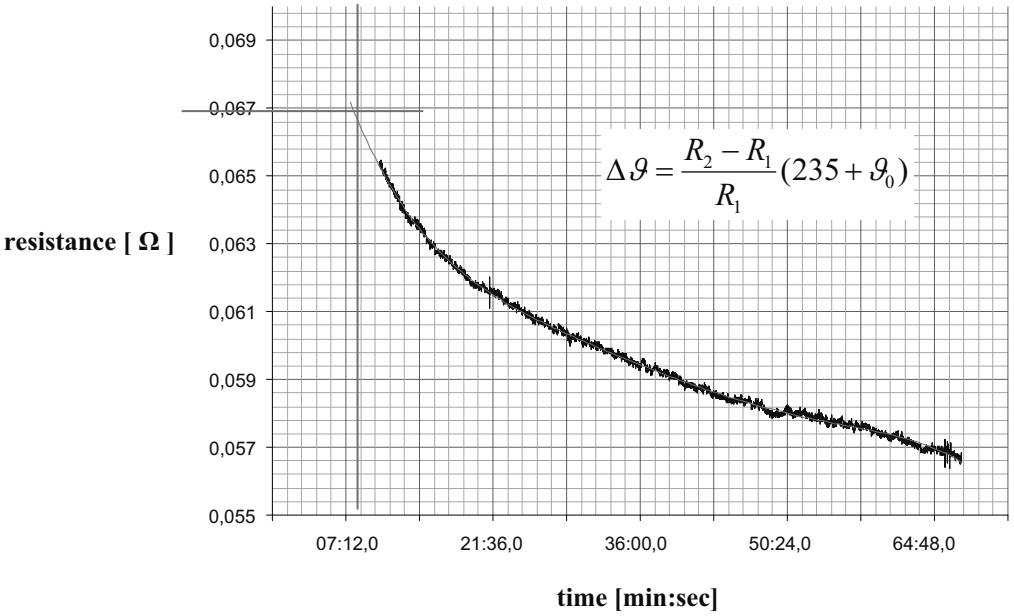

Figure 7: Cooling test – winding resistance, extrapolation to the point of switch off.

The machine moment of inertia J_p possibility of experimental determination is shown in Fig. 8. As was cited above it is necessary to find experimentally the speed-losses dependence for the correct evaluation of the moment of inertia. Finally, the moment of inertia can be determined from the length of subtangent T_{st} at known speed:

$$J_p = 91{,}2 \cdot \Delta P \cdot \frac{T_{st}}{n^2} \quad [\text{kgm}^2, \text{W}, \text{s}, \text{min}^{-1}]$$

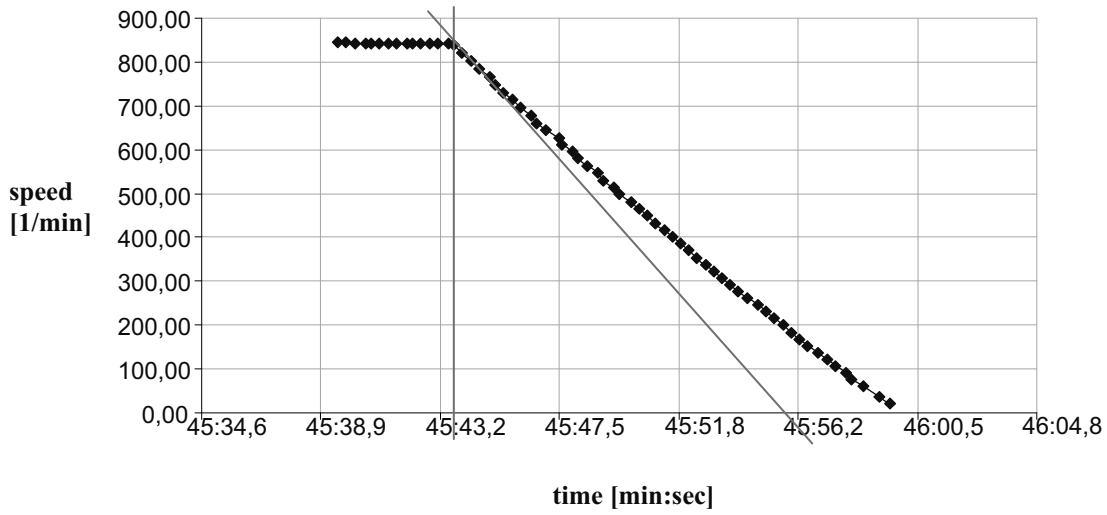

Figure 8: Retardation test for the moment of inertia determination.

6 CONCLUSION

The realized measurements confirm that an electric drive can be simulated like a rotating system on the basis of some above cited experimentally found characteristics knowing the vehicle running diagram and its load. The vehicle is then reduced to one driven axletree or to one wheel with in-built drive and a particular part of the total vehicle load which represents the dynamic torque. It is possible to realize the model, e.g., as a rotating set: motor – dynamometer (calibrated machine) – fly-wheel. It is possible to simulate the vehicle's operation on a given road profile at a given running mode and to verify the availability of the drive unit dimensioning.

REFERENCES

Bašta, J., Kulda, V., Měřička, J., 1959. *Měření na elektrických strojích*. Praha: SNTL. (in Czech)

Douda, P., Heptner, T., Kolář, J., 2002. *Pozemní dopravní prostředky*. Praha: ČVUT. (in Czech)

Gieras, J. F., Wing, M., 2002. *Permanent Magnet Motor Technology: design and application*. New York: Marcel Dekker. 590 p. ISBN 0-8247-0739-7.